Journal of Electrical Systems and Information Technology 1 (2014) 82–93
www.elsevier.com/locate/jesit

# Approximate electromagnetic cloaking of a conducting cylinder using homogeneous isotropic multi-layered materials

Hany M. Zamel [a,*], Essam El-Diwany [a], Hadia El-Hennawy [b]

[a] Microwave Engineering Department, Electronics Research Institute, Egypt
[b] Faculty of Engineering, Ain Shams University, Egypt

Available online 19 March 2014

**Abstract**

Cloaking refers to hiding a body from detection by surrounding it with a coating consisting of an unusual anisotropic nonhomogeneous material. Its function is to deflect the rays that would have struck the object, guide them around the object, and return them to their original trajectory, thus no waves are scattered from the body. The permittivity and permeability of such a cloak are determined by the coordinate transformation of compressing a hidden body into a point or a line. Some components of the electrical parameters of the cloaking material ($\varepsilon$, $\mu$) are required to have infinite or zero value at the boundary of the hidden object. Approximate cloaking can be achieved by transforming the cylindrical body (dielectric and conducting) virtually into a small cylinder rather than a line, which eliminates the zero or infinite values of the electrical parameters. The radially-dependent cylindrical cloaking shell can be approximately discretized into many homogeneous anisotropic layers; each anisotropic layer can be replaced by a pair of equivalent isotropic sub-layers, where the effective medium approximation is used to find the parameters of these two equivalent sub-layers. In this work, the scattering properties of cloaked perfectly conducting cylinder is investigated using a combination of approximate cloaking, together with discretizing the cloaking material using pairs of homogeneous isotropic sub-layers. The solution is obtained by rigorously solving Maxwell equations using angular harmonics expansion. The scattering pattern, and the back scattering cross section against the frequency are studied for both transverse magnetic ($TM_z$) and transverse electric ($TE_z$) polarizations of the incident plane wave for different transformed body radii.


*Keywords:* Approximate cloaking; Conducting cylinder; Cloaking by layered isotropic materials

## 1. Introduction

Recently, the concept of electromagnetic cloaking has drawn considerable attention concerning theoretical, numerical and experimental aspects (Pendry et al., 2006; Cheng et al., 2009; Yang et al., 2011; Shahzad et al., 2011; Cheng et al., 2010; Zhang and Mortensen, 2011; Zhai and Cui, 2011; Schurig et al., 2006). One approach to achieve electromagnetic

* Corresponding author.
*E-mail address:* hany@eri.sci.eg (H.M. Zamel).
Peer review under responsibility of Electronics Research Institute (ERI).

ELSEVIER Production and hosting by Elsevier

http://dx.doi.org/10.1016/j.jesit.2014.03.005

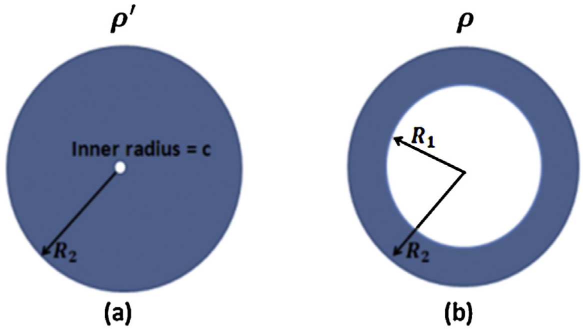


Fig. 1. (a) Virtual domain and (b) actual domain.

cloaking is to deflect the rays that would have struck the object, guide them around the object, and return them to their original trajectory, thus no waves are scattered from the body (Pendry et al., 2006). In the coordinate transformation method for cloaking, the body to be hidden is transformed virtually into a point (3D or spherical configuration) or a line (2D or cylindrical configuration), and this transformation leads to radially nonhomogeneous profiles of anisotropic permittivity and permeability $\varepsilon$, $\mu$ in the cloaking coating. One problem for the line-transformed cloaks is that some components of the parameters ($\varepsilon$, $\mu$) always have singularities at the inner boundary. For cylindrical cloak, $\varepsilon_\phi$, $\mu_\phi$ are infinite while $\varepsilon_\rho$, $\mu_\rho$, $\varepsilon_z$, $\mu_z$ are zero. This requires the use of metamaterials which can produce such values, however, they are narrow band since they rely on using array of resonant elements (as split ring resonators) (Pendry et al., 1999; Eleftheriades and Balmain, 2005; Engheta and Ziolkowski, 2006; Wang et al., 2009). To avoid the problem of the infinite or zero material parameters at the hidden body boundary, two approaches are studied. The first is removing a thin layer from the inner boundary; however, cloaking is very sensitive to this removal (Shahzad et al., 2011; Ruan et al., 2007). Another technique to obtain approximate cloaking is to transform the hidden body virtually into a small object rather than a point or a line as shown in Fig. 1, which eliminates the zero or infinite values of the electromagnetic parameters (Liu, 2009; Zhou, 2010; Song et al., 2012). This, however, leads to some scattering since the hidden body is virtually transformed into a small object rather than a point or a line, and the scattering decreases as the transformed cylinder radius is smaller.

The radially-dependent cylindrical cloaking shell can be approximately discretized into many homogeneous anisotropic layers, provided that the thickness of each layer is much less than the wavelength, and this discretization raises the level of scattering as the number of layers decreases. Each anisotropic layer can be replaced by a pair of equivalent homogeneous isotropic sub-layers A and B with different thicknesses, where the effective medium approximation is used to find the parameters of these two equivalent sub-layers (Huang et al., 2007). The combination of approximate cloaking with layered cloaking material is considered in (Song et al., 2012).

In this work, the scattering properties of cloaked perfectly conducting cylinder is investigated using a combination of approximate cloaking together with discretizing the cloaking material using pairs of homogeneous isotropic sub-layers. The solution is obtained by rigorously solving Maxwell equations using angular harmonics expansion. The scattering pattern, and the back scattering cross section against the frequency are studied for both $TM_z$ and $TE_z$ polarizations of the incident plane wave for different transformed body radii.

## 2. Coordinate transformation method for cloaking

### 2.1. Material parameters of the approximate cylindrical cloak

Perfect cylindrical cloak can be constructed by compressing the electromagnetic fields in a cylindrical region $\rho' \leq R_2$ into a cylindrical shell $R_1 \leq \rho \leq R_2$ as shown in Fig. 1. The coordinate transformation relates the radius $\rho'$ in the virtual domain to the corresponding radius $\rho$ in the cloaking material. The coordinate transformation is $\rho' = f(\rho)$, with $f(R_1) = 0$ for perfect cloaking or $f(R_1) = c$ for approximate cloaking and $f(R_2) = R_2$ (Zhou, 2010), while $\varphi$ and $z$ are kept unchanged, where $c$ is the reduced radius in the virtual domain. In the principal directions ($\rho$, $\varphi$, $z$ in cylindrical coordinates) this transformation leads to a diagonal Jacobian matrix $T$ (McGuirk, 2009; Hu et al., 2009):

$$T = \begin{bmatrix} Q_\rho & 0 & 0 \\ 0 & Q_\varphi & 0 \\ 0 & 0 & Q_z \end{bmatrix} \tag{1}$$

whose elements are the stretching ratios ($Q_\rho$, $Q_\varphi$, $Q_z$) of the line elements in the principal directions ($d\rho'/d\rho$, $\rho' d\varphi'/\rho d\varphi$, $dz'/dz$) in the virtual domain relative to the actual domain.

The radial and transverse permittivity and permeability of the cylindrical cloak, depending on $\rho$, are given as (Pendry et al., 2006; Yan et al., 2009):

$$\begin{aligned} \frac{\varepsilon_\rho}{\varepsilon_0} &= \frac{\mu_\rho}{\mu_0} = \frac{Q_\varphi Q_z}{Q_\rho} = \frac{f(\rho)}{\rho f'(\rho)} \\ \frac{\varepsilon_\varphi}{\varepsilon_0} &= \frac{\mu_\varphi}{\mu_0} = \frac{Q_\rho Q_z}{Q_\varphi} = \frac{\rho f'(\rho)}{f(\rho)} \\ \frac{\varepsilon_z}{\varepsilon_0} &= \frac{\mu_z}{\mu_0} = \frac{Q_\varphi Q_\rho}{Q_z} = \frac{f(\rho) f'(\rho)}{\rho} \end{aligned} \tag{2}$$

A linear transformation is usually used, given for approximate cloaking by (for ideal cloaking $c = 0$) (Zhou, 2010; Zamel et al., 2012):

$$f(\rho) = \rho' = \frac{1}{(R_2 - R_1)}[\rho(R_2 - c) + R_2(c - R_1)] \tag{3}$$

Thus, the permittivity and permeability of the approximate cylindrical cloak are given from the above equations by:

$$\frac{\varepsilon_\rho}{\varepsilon_0} = \frac{\mu_\rho}{\mu_0} = \frac{\rho(R_2 - c) + R_2(c - R_1)}{\rho(R_2 - c)} \tag{4}$$

$$\frac{\varepsilon_\varphi}{\varepsilon_0} = \frac{\mu_\varphi}{\mu_0} = \frac{\rho(R_2 - c)}{\rho(R_2 - c) + R_2(c - R_1)} \tag{5}$$

$$\frac{\varepsilon_z}{\varepsilon_0} = \frac{\mu_z}{\mu_0} = \frac{\rho(R_2 - c)^2 + R_2(c - R_1)(R_2 - c)}{\rho(R_2 - R_1)} \tag{6}$$

At $\rho = R_1$,

$$\frac{\varepsilon_\rho}{\varepsilon_0} = \frac{R_1(R_2 - c) + R_2(c - R_1)}{R_1(R_2 - c)} = \frac{c(R_2 - R_1)}{R_1(R_2 - c)} \tag{7}$$

$$\frac{\varepsilon_\varphi}{\varepsilon_0} = \frac{R_1(R_2 - c)}{R_1(R_2 - c) + R_2(c - R_1)} = \frac{R_1(R_2 - c)}{c(R_2 - R_1)} \tag{8}$$

$$\frac{\varepsilon_z}{\varepsilon_0} = \frac{R_1(R_2 - c)^2 + R_2(c - R_1)(R_2 - c)}{R_1(R_2 - R_1)^2} = \frac{c(R_2 - c)}{R_1(R_2 - R_1)} \tag{9}$$

For approximate cloaking $\varepsilon_\varphi$, $\mu_\varphi$ are proportional to $1/c$, while $\varepsilon_\rho$, $\mu_\rho$, $\varepsilon_z$, $\mu_z$ are proportional to $c$. Thus, for ideal cloaking ($c = 0$), at the inner boundary, $\varepsilon_\varphi$, $\mu_\varphi$ are infinitely large, and the other components are zero.

At $\rho = R_2$,

$$\frac{\varepsilon_\rho}{\varepsilon_0} = \frac{R_2 - R_1}{R_2 - c} \tag{10}$$

$$\frac{\varepsilon_\varphi}{\varepsilon_0} = \frac{R_2 - c}{R_2 - R_1} \tag{11}$$

$$\frac{\varepsilon_z}{\varepsilon_0} = \frac{(R_2 - c)^2 + (c - R_1)(R_2 - c)}{(R_2 - R_1)^2} = \frac{R_2 - c}{(R_2 - R_1)} \tag{12}$$

The fields $E^i = [E^i_\rho, E^i_\varphi, E^i_z]$ and $H^i = [H^i_\rho, H^i_\varphi, H^i_z]$ in the virtual domain are related to the fields in the cloak medium $\widehat{E}$, $\widehat{H}$ by the relation $\widehat{E} = T^t E^i$. For cylindrical cloaks (Yan et al., 2009)

$$\hat{E}_\rho = f'(\rho)E^i_\rho(f(\rho), \varphi, z),\ \hat{H}_\rho = f'(\rho)H^i_\rho(f(\rho), \varphi, z) \tag{13}$$

$$\hat{E}_\phi = \frac{f(\rho)}{\rho}E^i_\phi(f(\rho), \phi, z),\ \hat{H}_\phi = \frac{f(\rho)}{\rho}H^i_\phi(f(\rho), \phi, z) \tag{14}$$

$$\hat{E}_z = E^i_z(f(\rho), \phi, z),\ \hat{H}_z = H^i_z(f(\rho), \phi, z) \tag{15}$$

## 3. Formulation of the problem of scattering by cylindrical layered structure of homogeneous isotropic materials

The radially-dependent cylindrical cloaking shell can be approximately discretized into many homogeneous anisotropic layers, provided that the thickness of each layer is much less than the wavelength, and this discretization raises the level of scattering as the number of layers decreases. Each anisotropic layer can be replaced by a pair of equivalent homogeneous isotropic sub-layers A and B with different thicknesses, where the effective medium approximation is used to find the parameters of these two equivalent sub-layers (Huang et al., 2007), as shown in Fig. 2.

To study fields and waves in cylindrical coordinates, the normally incident field on the cylinder can be decomposed into $TE_z$ and $TM_z$ fields w.r.t. the axial $\hat{z}$ direction. Thus, for $TE_z$ fields only $\mu_z$, $\varepsilon_\rho$ and $\varepsilon_\varphi$ are required when analyzing field behaviour. $TM_z$ fields require $\varepsilon_z$, $\mu_\rho$ and $\mu_\varphi$.

### 3.1. The parameters of the isotropic layers

When the layer thicknesses ($d_A$, $d_B$) are much less than the wavelength λ, the relationships between the anisotropic permittivities $\varepsilon_\rho$, $\varepsilon_\varphi$ and the two-layer isotropic permittivities $\varepsilon_A$, $\varepsilon_B$ for $TE_z$ polarization are given by Huang et al. (2007):

$$\varepsilon_\rho = \frac{(1+\eta)\varepsilon_A\varepsilon_B}{\varepsilon_B + \eta\varepsilon_A} \tag{16}$$

$$\varepsilon_\varphi = \frac{\varepsilon_A + \eta\varepsilon_B}{1+\eta} \tag{17}$$

In which, $\eta = d_B/d_A$, $d_A$ and $d_B$ are the thicknesses of the layers A and B, respectively. These formulas correspond to series and parallel combinations of capacitors of layers A and B in the $r$- and $\varphi$-directions.

By solving the above equations for $\varepsilon_A$ and $\varepsilon_B$, one can obtain the equivalent medium parameters for the isotropic sub-layers when the thicknesses are identical ($\eta = 1$):

$$\varepsilon_B = \varepsilon_\varphi + \sqrt{\varepsilon_\varphi^2 - \varepsilon_\varphi\varepsilon_\rho} \tag{18}$$

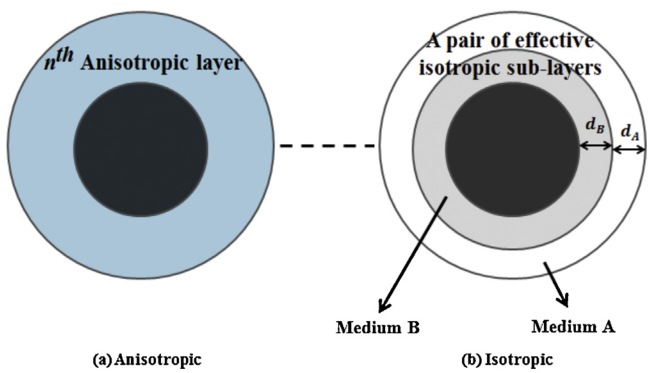


Fig. 2. Equivalence of an anisotropic cylindrical shell and two isotropic sub-shells.

$$\varepsilon_A = \varepsilon_\varphi - \sqrt{\varepsilon_\varphi^2 - \varepsilon_\varphi \varepsilon_\rho} \tag{19}$$

which are used together with the axial permeability $\mu_z$. Similar expressions hold for $\mu$ for $TM_z$ polarization. The values of $\varepsilon_\varphi$, $\varepsilon_\rho$ and $\mu_z$ are taken at the average radius of the layer.

### 3.2. Scattering by a cloaked cylinder

The configuration for electromagnetic scattering by the cylindrical body (dielectric and conducting) coated by 2 M layers is shown in Fig. 3. The external radius, permittivity, and permeability of the core and the layers are denoted by $a_i$, $\varepsilon_i$ and $\mu_i$ ($i = 1, 2, \ldots, 2M+1$), respectively. Fig. 3 shows an $E_z$ polarized plane wave with amplitude $E_0$, $E^{\text{inc}} = E_0 e^{-jK_0 x}\hat{z}$, incident upon the coated cylinder along the $\hat{x}$ direction, where $k_0 = \omega\sqrt{\varepsilon_0 \mu_0}$, $j = \sqrt{-1}$. The time dependence of $e^{j\omega t}$ is suppressed. The incident field can be expanded in angular harmonics for $TM_z$ and $TE_z$ polarizations as (Jin, 2010):

$$E_z^{inc} = E_0 \sum_{n=-\infty}^{\infty} (j)^{-n} J_n(k_0\rho) e^{jn\varphi} \tag{20}$$

$$H_z^{inc} = H_0 \sum_{n=-\infty}^{\infty} (j)^{-n} J_n(k_0\rho) e^{jn\varphi} \tag{21}$$

where $J_n$ is the $n^{\text{th}}$ order Bessel function of the first kind, $n$ is integer.

The scattered $E_z^S$ field for $TM_z$ polarization can be expanded as (Jin, 2010):

$$E_z^S = E_0 \sum_{n=-\infty}^{\infty} (j)^{-n} A_n H_n^2(k_0\rho) e^{jn\varphi} \tag{22}$$

Also, the scattered field $H_z^S$ for $TE_z$ polarization can be expanded as:

$$H_z^S = H_0 \sum_{n=-\infty}^{\infty} (j)^{-n} B_n H_n^2(k_0\rho) e^{jn\varphi} \tag{23}$$

where $H_n^2$ is the $n^{\text{th}}$ order Hankel function of the second kind, $A_n$ and $B_n$ are coefficients to be determined.

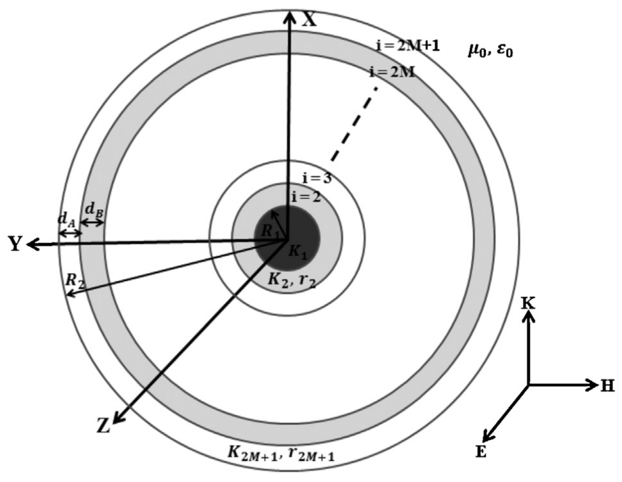


Fig. 3. Plane wave scattering by a multilayer dielectric cylinder.

For TM$_z$ polarization, the field in the $i^{\text{th}}$ layer can be expressed as:

$$E_z^i = E_0 \sum_{n=-\infty}^{\infty} (j)^{-n} \left[ C_n^i H_n^1(k_i\rho) + D_n^i H_n^2(k_i\rho) \right] e^{jn\phi} \tag{24}$$

where $k_i = \omega\sqrt{\varepsilon_i \mu_i}$.

From Maxwell equation

$$H_\varphi^i = \frac{1}{j\mu\omega} \frac{\partial E_z^i}{\partial \rho} \tag{25}$$

Hence, for TM$_z$ polarization (Jin, 2010):

$$H_\varphi^i = \frac{E_0}{j\eta_i} \sum_{n=-\infty}^{\infty} (j)^{-n} \left[ C_n^i \left[H_n^1(k_i\rho)\right]' + D_n^i \left[H_n^2(k_i\rho)\right]' \right] e^{jn\varphi} \tag{26}$$

where $\eta_j = \sqrt{\mu_i/\varepsilon_i}$, and the prime over the square bracket indicates differentiation w.r.t. the argument.

For TE$_z$ polarization, the field in the $i^{\text{th}}$ layer can be expressed as:

$$H_z^i = H_0 \sum_{n=-\infty}^{\infty} (j)^{-n} [\tilde{C}_n^i H_n^1(k_i\rho) + \tilde{D}_n^i H_n^2(k_i\rho)] e^{jn\varphi} \tag{27}$$

From Maxwell equation:

$$E_\varphi^i = \frac{-1}{j\omega\varepsilon} \frac{\partial H_z^i}{\partial \rho} \tag{28}$$

Hence,

$$E_\varphi^i = jH_0\eta_i \sum_{n=-\infty}^{\infty} (j)^{-n} \left[ \tilde{C}_n^i \left[H_n^1(k_i\rho)\right]' + \tilde{D}_n^i \left[H_n^2(k_1\rho)\right]' \right] e^{jn\varphi} \tag{29}$$

For TM$_z$ polarization, the boundary conditions are that the tangential components $E_z$ and $H_\varphi$, respectively, are continuous across the cylindrical interfaces $\rho = a_i$ $(i = 1, 2, \ldots, 2M)$ and can be expressed as:

$$C_n^{i+1} H_n^1(k_{i+1}a_i) + D_n^{i+1} H_n^2(k_{i+1}a_i) = C_n^i H_n^1(k_i a_i) + D_n^i H_n^2(k_i a_i) \tag{30}$$

$$\sqrt{\frac{\varepsilon_{i+1}}{\mu_{i+1}}} \left[ C_n^{i+1} \left[H_n^1(k_{i+1}a_i)\right]' + D_n^{i+1} \left[H_n^2(k_{i+1}a_i)\right]' \right] = \sqrt{\frac{\varepsilon_i}{\mu_i}} \left[ C_n^i \left[H_n^1(k_i a_i)\right]' + D_n^i \left[H_n^2(k_i a_i)\right]' \right] \tag{31}$$

For TE$_z$ polarization, the boundary conditions are that the tangential components $H_z$ and $E_\varphi$, respectively, are continuous across the cylindrical interfaces $\rho = a_i (i = 1, 2, ..., 2M)$ and can be expressed as:

$$\left[ \tilde{C}_n^{i+1} H_n^1(k_{i+1}a_i) + \tilde{D}_n^{i+1} H_n^2(k_{i+1}a_i) \right] = \left[ \tilde{C}_n^i H_n^1(k_i a_i) + \tilde{D}_n^i H_n^2(k_i a_i) \right] \tag{32}$$

$$\sqrt{\frac{\mu_{i+1}}{\varepsilon_{i+1}}} \left[ \tilde{C}_n^{i+1} \left[H_n^1(k_{i+1}a_i)\right]' + \tilde{D}_n^{i+1} \left[H_n^2(k_{i+1}a_i)\right]' \right] = \sqrt{\frac{\mu_i}{\varepsilon_i}} \left[ \tilde{C}_n^i \left[H_n^1(k_i a_i)\right]' + \tilde{D}_n^i \left[H_n^2(k_i a_i)\right]' \right] \tag{33}$$

The finiteness of the field in the dielectric core leads to the following ratios in the dielectric core (Jin, 2010):

$$\frac{D_n^1}{C_n^1} = 1, \; \frac{\tilde{D}_n^1}{\tilde{C}_n^1} = 1 \tag{34}$$

When cloaking a conducting cylinder, the dielectric constant in the core is taken to be very large.

The ratios $D_n^{i+1}/C_n^{i+1}$ and $\tilde{D}_n^{i+1}/\tilde{C}_n^{i+1}$ in the successive larger layers can be obtained iteratively from the following equations (Jin, 2010):

$$\frac{D_n^{i+1}}{C_n^{i+1}} = -\frac{H_n^1(k_{i+1}a_i) - R_E^i H_n^{1'}(k_{i+1}a_i)}{H_n^2(k_{i+1}a_i) - R_E^i H_n^{2'}(k_{i+1}a_i)}, \quad i = 1, 2, \ldots, 2M \tag{35}$$

$$\frac{\tilde{D}_n^{i+1}}{\tilde{C}_n^{i+1}} = -\frac{H_n^1(k_{i+1}a_i) - R_H^i H_n^{1'}(k_{i+1}a_i)}{H_n^2(k_{i+1}a_i) - R_H^i H_n^{2'}(k_{i+1}a_i)}, \quad i = 1, \ldots, 2M \tag{36}$$

where

$$R_E^i = \sqrt{\frac{\mu_i \varepsilon_{i+1}}{\varepsilon_i \mu_{i+1}}} \frac{H_n^1(k_i a_i) + \frac{D_n^i}{C_n^i} H_n^2(k_i a_i)}{H_n^{1'}(k_i a_i) + \frac{D_n^i}{C_n^i} H_n^{2'}(k_i a_i)}, \quad i = 1, 2, \ldots, 2M \tag{37}$$

$$R_H^i = \sqrt{\frac{\mu_{i+1} \varepsilon_i}{\varepsilon_{i+1} \mu_i}} \frac{H_n^1(k_i a_i) + \frac{\tilde{D}_n^i}{\tilde{C}_n^i} H_n^2(k_i a_i)}{H_n^{1'}(k_i a_i) + \frac{\tilde{D}_n^i}{\tilde{C}_n^i} H_n^{2'}(k_i a_i)}, \quad i = 1, 2, \ldots, 2M \tag{38}$$

Finally, the boundary conditions between the outer layer and air lead to the following equations:

$$J_n(k_0 R_2) + A_n H_n^2(k_0 R_2) = C_n^{2M+1} H_n^1(k_{2M+1} R_2) + D_n^{2M+1} H_n^2(k_{2M+1} R_2) \tag{39}$$

$$\sqrt{\frac{\varepsilon_0}{\mu_0}} \left[ [J_n(k_0 R_2)]' + A_n \left[ H_n^2(k_0 R_2) \right]' \right] = \sqrt{\frac{\varepsilon_{2M+1}}{\mu_{2M+1}}} \left[ C_n^{2M+1} \left[ H_n^1(k_{2M+1} R_2) \right]' + D_n^{2M+1} \left[ H_n^2(k_{2M+1} R_2) \right]' \right] \tag{40}$$

$$J_n(k_0 R_2) + B_n H_n^2(k_0 R_2) = \tilde{C}_n^{2M+1} H_n^1(k_{2M+1} R_2) + \tilde{D}_n^{2M+1} H_n^2(k_{2M+1} R_2) \tag{41}$$

$$\sqrt{\frac{\mu_0}{\varepsilon_0}} \left[ [J_n(k_0 R_2)]' + B_n \left[ H_n^2(k_0 R_2) \right]' \right] = \sqrt{\frac{\mu_{2M+1}}{\varepsilon_{2M+1}}} \left[ \tilde{C}_n^{2M+1} \left[ H_n^1(k_{2M+1} R_2) \right]' + \tilde{D}_n^{2M+1} \left[ H_n^2(k_{2M+1} R_2) \right]' \right] \tag{42}$$

From these equations, we can get the scattering coefficients $A_n$ ($\text{TM}_z$ case) and $B_n$ ($\text{TE}_z$ case):

$$A_n = -\frac{J_n(k_0 R_2) - R_E^{2M+1} J_n'(k_0 R_2)}{H_n^2(k_0 R_2) - R_E^{2M+1} H_n^{2\prime}(k_0 R_2)} \tag{43}$$

$$B_n = -\frac{J_n(k_0 R_2) - R_H^{2M+1} J_n'(k_0 R_2)}{H_n^2(k_0 R_2) - R_H^{2M+1} H_n^{2'}(k_0 R_2)} \tag{44}$$

The mode series is truncated at the mode number $n_{\max} = k_0 R_2 + 5$ (Li and Shen, 2003).

### 3.3. The scattering width

For the 2-D scattering problem, the scattering width $\sigma(\varphi)$, which is referred to as the scattering cross section per unit length, is defined as (Ruck et al., 1970):

$$\sigma(\varphi) = \lim_{\rho \to \infty} 2\pi\rho \frac{|E^S(\varphi)|^2}{|E^i|^2} = \lim_{\rho \to \infty} 2\pi\rho \frac{|H^S(\varphi)|^2}{|H^i|^2} \tag{45}$$

The scattering width $\sigma(\varphi)$ defines the scattering in an arbitrary direction (for forward scattering $\varphi = 0°$, for back scattering $\varphi = \pi$).

For $\text{TM}_z$ case (Ruck et al., 1970):

$$\sigma(\phi) = \frac{4}{k_0} \left| \sum_{n=0}^{\infty} (-1)^n \varepsilon_n A_n \cos(n\phi) \right|^2 \tag{46}$$

For $TE_z$ case (Ruck et al., 1970):

$$\sigma(\phi) = \frac{4}{k_0}\left|\sum_{n=0}^{\infty}(-1)^n \varepsilon_n B_n \cos(n\phi)\right|^2 \tag{47}$$

where the Neuman number

$$\varepsilon_n = \begin{cases} 1 & \text{for} \quad n = 0 \\ 2 & \text{for} \quad n = 1, 2, 3, \ldots \end{cases}$$

## 4. Results

To check the above analysis, the far field scattering pattern for a bare conducting cylinder shelled with 2 M layers of alternating dielectric A and B with identical thickness ($\eta = 1$) are calculated for $M = 5$, 20, and compared with the results in (Huang et al., 2007), leading to identical results.

### 4.1. Normalized bistatic scattering width

To show the effect of the cloaking radius c on the normalized bistatic scattering width, consider the inner core with radius $R_1 = \lambda$, the outermost radius $R_2 = 2R_1$, where $\lambda$ is the wavelength, the cloak is discretized into $2M = 40$ layers. Figs. 4 and 5 show the normalized bistatic scattering width ($\sigma/R_1$) versus the angle $\varphi$ of cloaked conducting cylinder coated with multilayered isotropic homogenous layers for the ideal ($c = 0$) and three different cloaking radii $c$ for $TE_z$ and $TM_z$ cases, respectively. It can be seen from Figs. 4 and 5 that, use of approximate cloaking ($c = R_1/10$, $R_1/20$ and $R_1/40$) leads to reduction of the scattering compared with the uncoated conducting cylinder. The scattering from the layered cloak shows high endfire scattering ($\varphi = 0°$), similar to the behaviour of scattering from the uncloaked cylinder.

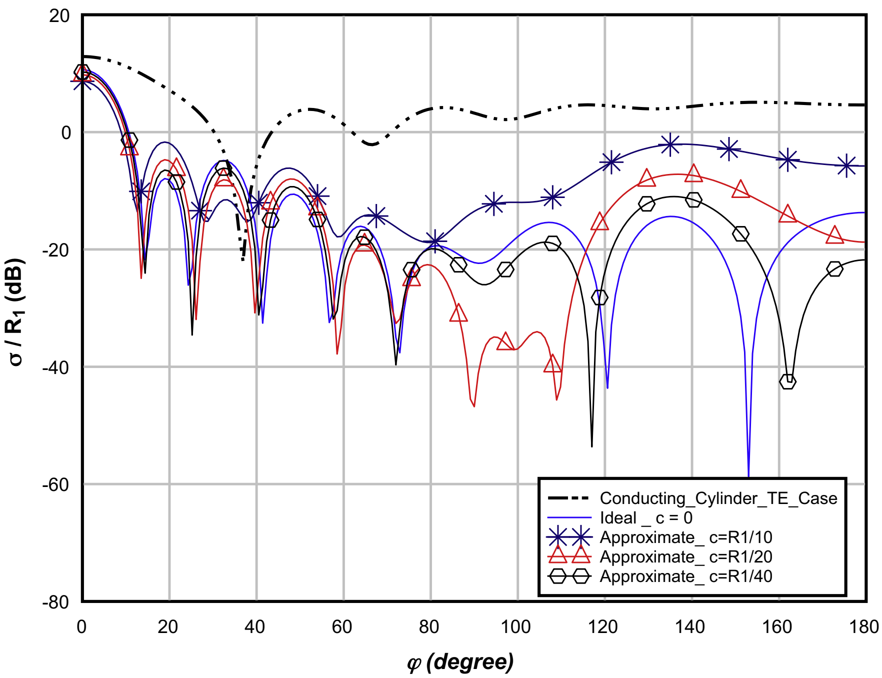


Fig. 4. Normalized bistatic scattering width for cloaked conducting cylinder with multilayered isotropic structure for different reduced radii, $TE_z$ case.

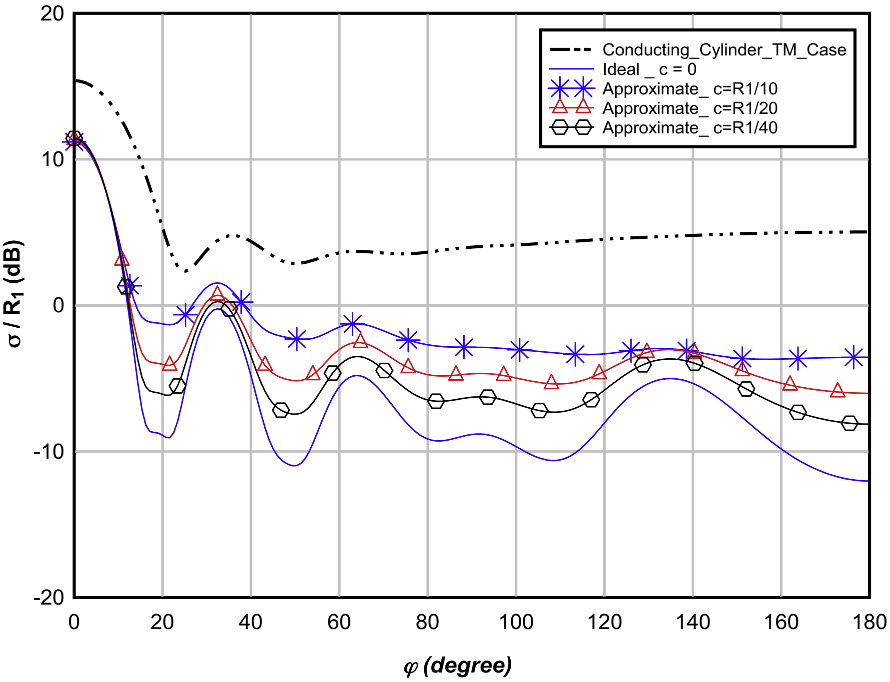


Fig. 5. Normalized bistatic scattering width for cloaked conducting cylinder with multilayered isotropic structure for different reduced radii, $TM_z$ case.

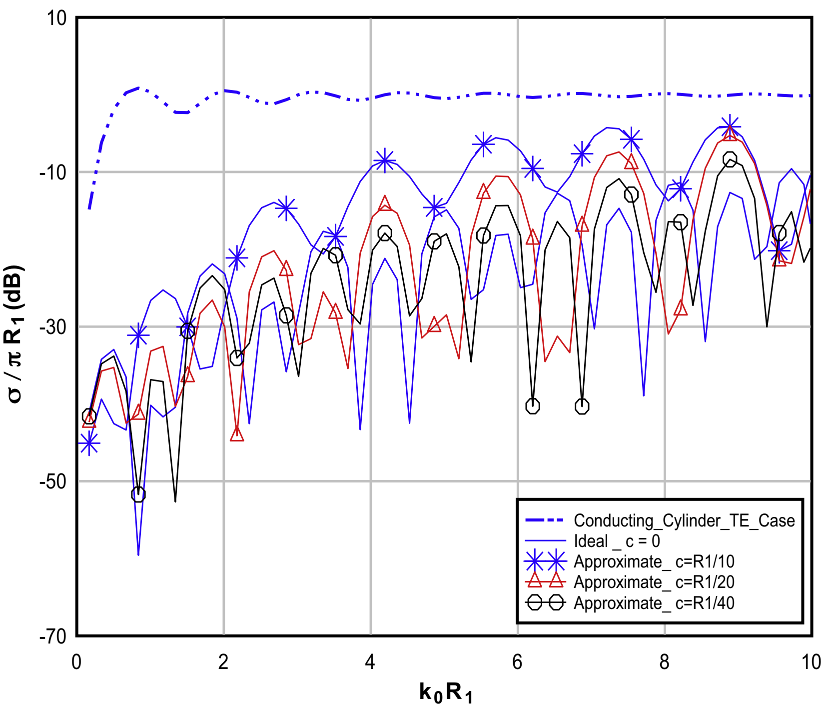


Fig. 6. Normalized back scattering width for cloaked conducting cylinder with multilayered isotropic structure for different reduced radii, $TE_z$ case.

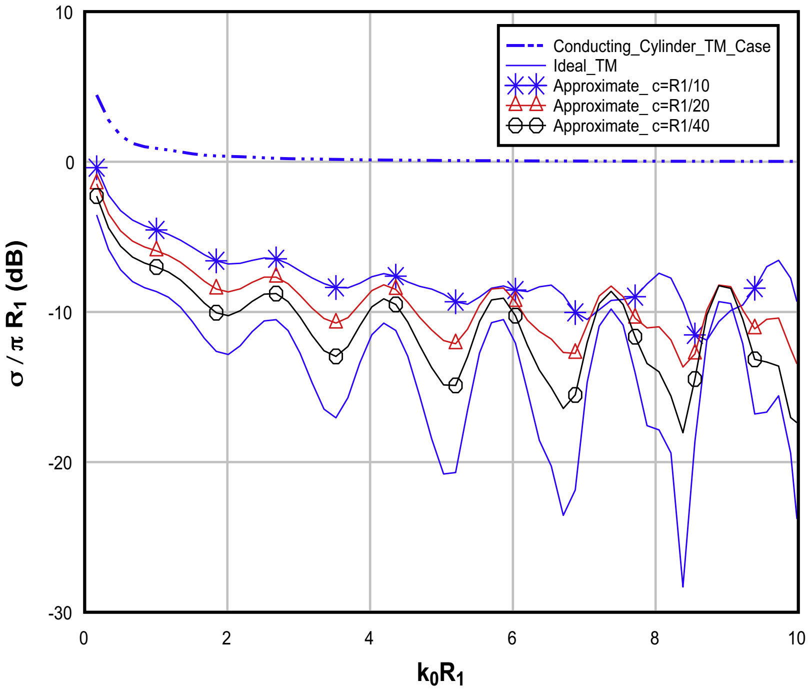


Fig. 7. Normalized back scattering width for cloaked conducting cylinder with multilayered isotropic structure for different reduced radii, $TM_z$ case.

### 4.2. *Normalized back scattering width*

Figs. 6 and 7 show the normalized back scattering width ($\sigma/\pi R_1$) versus the normalized frequency $k_0R_1$ for cloaked conducting cylinder coated with multi isotropic homogenous layers ($R_2 = 2R_1$, $2M = 40$), for the ideal ($c = 0$) and three different cloaking radii c for $TE_z$ and $TM_z$ cases, respectively. It can be seen from Figs. 6 and 7 that when the reduced radius $c$ decreases, the back scattering width decreases on the average. By setting $c = R_1/40$ the scattering approaches that of the ideal profile $c = 0$. The back scattering width at low frequencies for $TE_z$ case increases generally as the frequency increases, similar to the behaviour of the scattering by the conducting cylinder, which results from the reflected and creeping waves. On the other hand, the back scattering width at low frequencies for $TM_z$ case decreases generally as the frequency increases, similar to the behaviour of the scattering by the conducting cylinder, which is high at low frequencies, since the incident electric field is parallel to the cylinder. The reduction of scattering by cloaking at low frequencies, compared with the uncloaked conducting cylinder, is more significant for $TE_z$ polarization than for $TM_z$ polarization.

### 4.3. *Permittivity and permeability profiles in the cloak layers*

Fig. 8 shows values of the relative permittivity in the cloaking layers for perfect cloaking $c = 0$ and two different radii for approximate cloaks, Eqs. (4), (5), (18), and (19). We consider $R_2 = 2R_1$ and the cloak is discretized into $2M = 40$ layers. For the ideal case, the value of the relative permittivity $\varepsilon_\varphi$ at the inner boundary approaches infinity, Eq. (8), but for approximate cloaking the value of $\varepsilon_B/\varepsilon_0$ at the inner layer is finite (53 for $c = R_1/20$ and 80 for $c = R_1/40$), Eqs. (7), (8), (18), as shown in Fig. 8. For ideal cloak ($c = 0$), $\mu_z$ is zero at the inner boundary, Eq. (9), but for approximate cloaking the value of the relative permeability ($\mu_z/\mu_0$) is finite (0.18 for $c = R_1/20$ and 0.14 for $c = R_1/40$).

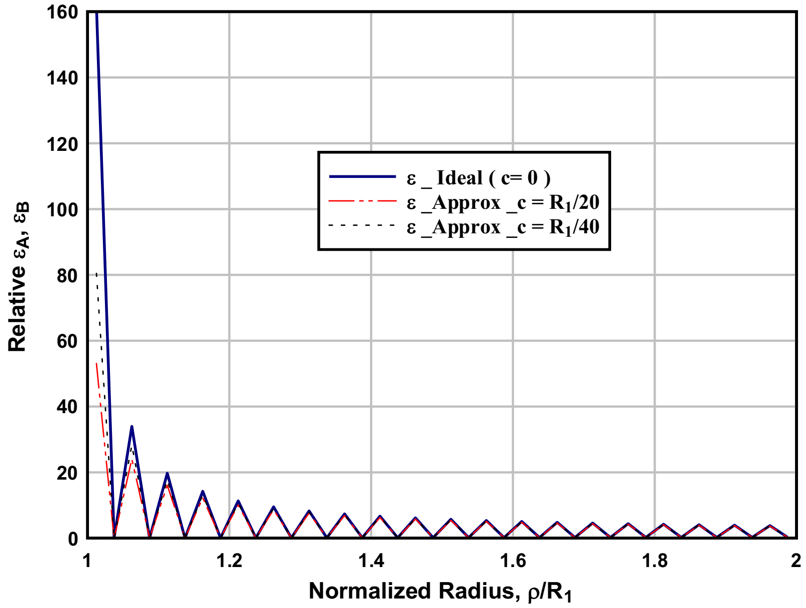


Fig. 8. Relative permittivities $\varepsilon_{A,B}$ in the layers for the multilayered isotropic structure.

## 5. Conclusion

In this work, the scattering from cloaked conducting cylindrical is studied for both $TE_z$ and $TM_z$ polarizations using approximate multilayer cloak of isotropic homogenous layers. The anisotropic transverse components of $\varepsilon(\mu)$ for $TE_z$ ($TM_z$) case are replaced by two isotropic layers, together with the single component of $\mu(\varepsilon)$. The solution is obtained iteratively for the angular modes amplitudes in the layers. The effect of approximate cloaking on removing the singular values of $\varepsilon$, $\mu$ components at the inner cloak radius shows that the components $\varepsilon_\varphi$, $\mu_\varphi$ vary as $\frac{R_1(R_2-c)}{c(R_2-R_1)}$, while the components $\varepsilon_\rho$, $\mu_\rho$ vary as $\frac{c(R_2-R_1)}{R_1(R_2-c)}$, and the components $\varepsilon_z$, $\mu_z$ vary as $\frac{c(R_2-c)}{R_1(R_2-R_1)}$. The scattering from the layered cloak shows high endfire scattering. The use of approximate cloaking leads to reduction of scattering compared with the uncoated conducting cylinder, particularly for $TE_z$ polarization at low frequencies. The back scattering versus frequency decreases on the average as the cloaking radius $c$ decreases.

## References

Cheng, Q., Jiang, W.X., Cui, T.J., 2009. Investigations of the electromagnetic properties of three-dimensional arbitrarily-shaped cloaks. Progr. Electromagnetics Res. 94, 105–117.
Cheng, X.X., Chen, H.S., Zhang, X.M., 2010. Cloaking a perfectly conducting sphere with rotationally uniaxial nihility media in monostatic radar system. Progr. Electrom. Res. M 100, 285–298.
Eleftheriades, G.V., Balmain, K.G., 2005. Negative Refraction Metamaterials – Fundamental Principles and Applications. John Wiley.
Engheta, N., Ziolkowski, R.W., 2006. Metamaterials: Physics and Engineering Explorations. Wiley-IEEE Press.
Hu, J., Zhou, X., Hu, G., 2009. Design method for electromagnetic cloak with arbitrary shapes based on Laplace's equation. Opt. Express 17 (15), 13070.
Huang, Y., Feng, Y., Jiang, T., 2007. Electromagnetic cloaking by layered structure of homogenous isotropic materials. Opt. Express 15 (18), 047602-1–047602-4.
Jin, J., 2010. Theory and Computation of Electromagnetic Fields. John Wiley.
Li, C., Shen, Z., 2003. Electromagnetic scattering by a conducting cylinder coated with metamaterials. Progr. Electrom. Res. 42, 91–105.
Liu, H., 2009. Virtual reshaping and invisibility in obstacle scattering. Inverse Probl. 25 (4), 1–10.
McGuirk, J., (Ph.D. thesis) 2009. Electromagnetic Field Control and Optimization Using Metamaterials. Air University, Ohio, USA.
Pendry, J.B., Holden, A.J., Robbins, D.J., Stewart, W.J., 1999. Magnetism from conductors and enhanced nonlinear phenomena. IEEE Trans. Micro. Theory Tech. 47 (11), 2075–2084.
Pendry, J.B., Schurig, D., Smith, D.R., 2006. Controlling electromagnetic fields. Science 312, 1780–1782.
Ruan, Z., Yan, M., Neff, C.W., Qiu, M., 2007. Ideal cylindrical cloak: perfect but sensitive to tiny perturbations. Phys. Rev. Let. 99, 113903.
Ruck, G.T., Barrick, D.E., Stuart, W.D., Krichbaum, C.K., 1970. Radar Cross Section Handbook. Kluwer Academic.

Schurig, D., Mock, J.J., Justice, B.J., Cummer, S.A., Pendry, J.B., Starr, A.F., Smith, D.R., 2006. Metamaterial electromagnetic cloak at microwave frequencies. Science 314, 977–980.

Shahzad, A., Qasim, F., Ahmed, S., Naqvi, Q.A., 2011. Cylindrical invisibility cloak incorporating PEMC at perturbed void region. Progr. Electrom. Res. M 21, 61–76.

Song, W., Yang, X., Sheng, X., 2012. Scattering characteristics of 2-D imperfect cloaks with layered isotropic materials. IEEE Antennas Propag. Let. 11, 53–56.

Wang, J., Qu, S., Zhang, J., Ma, H., Yang, Y., Gu, C., Wu, X., Xu, Z., 2009. A tunable left-handed metamaterial based on modified broadside-coupled split-ring resonators. Progr. Electrom. Res. Lett. 6, 35–45.

Yan, M., Yan, W., Qiu, M., 2009. Invisibility cloaking by coordinate transformation. Progr. Optics 52, 261–304.

Yang, J.J., Huang, M., Li, Y.L., Li, T.H., Sun, J., 2011. Reciprocal invisible cloak with homogeneous metamaterials. Progr. Electrom. Res. M 21, 105–115.

Zamel, H., El-Diwany, E., El-Hennawy, H., 2012. Approximate electromagnetic cloaking of spherical bodies. In: 29th National Radio Science Conference (NRSC), Egypt, pp. 19–28.

Zhai, Y.B., Cui, T.J., 2011. Three-dimensional axisymmetric invisibility cloaks with arbitrary shapes in layered-medium background. Progr. Electrom. Res. B 27, 151–163.

Zhang, J., Mortensen, N.A., 2011. Ultrathin cylindrical cloak. Progr. Electrom. Res. 121, 381–389.

Zhou, T., (Ph.D. thesis) 2010. Electromagnetic Inverse Problems and Cloaking. Washington University.